research communications

CRYSTALLOGRAPHIC COMMUNICATIONS
ISSN 2056-9890

Crystal structure of strontium dinickel iron orthophosphate

Said Ouaatta,* Abderrazzak Assani, Mohamed Saadi and Lahcen El Ammari

Laboratoire de Chimie du Solide Appliquée, Faculté des Sciences, Université Mohammed V, Avenue Ibn Battouta, BP 1014, Rabat, Morocco. *Correspondence e-mail: saidouaatta87@gmail.com

Received 9 September 2015
Accepted 22 September 2015

Edited by T. J. Prior, University of Hull, England

Keywords: crystal structure; transition metal phosphates; solid-state reaction synthesis; $SrNi_2Fe(PO_4)_3$; α-chromium phosphate

CCDC reference: 1426730
Supporting information: this article has supporting information at journals.iucr.org/e

The title compound, $SrNi_2Fe(PO_4)_3$, synthesized by solid-state reaction, crystallizes in an ordered variant of the α-$CrPO_4$ structure. In the asymmetric unit, two O atoms are in general positions, whereas all others atoms are in special positions of the space group *Imma*: the Sr cation and one P atom occupy the Wyckoff position 4*e* (*mm*2), Fe is on 4*b* (2/*m*), Ni and the other P atom are on 8*g* (2), one O atom is on 8*h* (*m*) and the other on 8*i* (*m*). The three-dimensional framework of the crystal structure is built up by [PO_4] tetrahedra, [FeO_6] octahedra and [Ni_2O_{10}] dimers of edge-sharing octahedra, linked through common corners or edges. This structure comprises two types of layers stacked alternately along the [100] direction. The first layer is formed by edge-sharing octahedra ([Ni_2O_{10}] dimer) linked to [PO_4] tetrahedra *via* common edges while the second layer is built up from a strontium row followed by infinite chains of alternating [PO_4] tetrahedra and FeO_6 octahedra sharing apices. The layers are held together through vertices of [PO_4] tetrahedra and [FeO_6] octahedra, leading to the appearance of two types of tunnels parallel to the *a*- and *b*-axis directions in which the Sr cations are located. Each Sr cation is surrounded by eight O atoms.

1. Chemical context

Phosphates with the alluaudite (Moore, 1971) and α-$CrPO_4$ (Attfield *et al.*, 1988) crystal structures have attracted great interest due to their potential applications as battery electrodes (Trad *et al.*, 2010; Kim *et al.*, 2014; Huang *et al.*, 2015). In the last decade, our interest has focused on those two phosphate derivatives and we have succeeded in synthesizing and structurally characterizing new phosphates such as $Na_2Co_2Fe(PO_4)_3$ (Bouraima *et al.*, 2015) and $Na_{1.67}Zn_{1.67}Fe_{1.33}(PO_4)_3$ (Khmiyas *et al.*, 2015) with the alluaudite structure type, and $MMn^{II}{}_2Mn^{III}(PO_4)_3$ (M = Pb, Sr, Ba) (Alhakmi *et al.* (2013*a*,*b*; Assani *et al.*, 2013) which belongs to the α-$CrPO_4$ structure type. In the same context, our solid-state chemistry investigations within the ternary system MO–M'O–NiO–P_2O_5 (M and M' are divalent cations), have led to the synthesis of the title compound $SrNi_2Fe(PO_4)_3$ which has a related α-$CrPO_4$ structure.

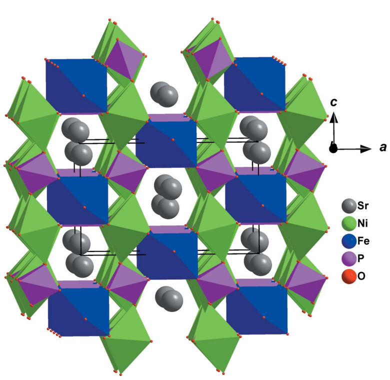

2. Structural commentary

The crystal structure of the title phosphate is formed by [PO_4] tetrahedra linked to [NiO_6] and [FeO_6] octahedra, as shown in Fig. 1. The octahedral environment of iron is more distorted than that of nickel (see Table 1). In this model, bond-valence-sum calculations (Brown & Altermatt, 1985) for Sr^{2+}, Ni^{2+}, Fe^{3+}, $P1^{5+}$and $P2^{5+}$ ions are as expected, *viz.* 1.88, 1.95, 2.91, 5.14 and 5.01 valence units, respectively. Atoms Sr1 and P1 occupy Wyckoff positions 4*e* (*mm*2), Fe1 is on 4*b* (2/*m*), Ni1

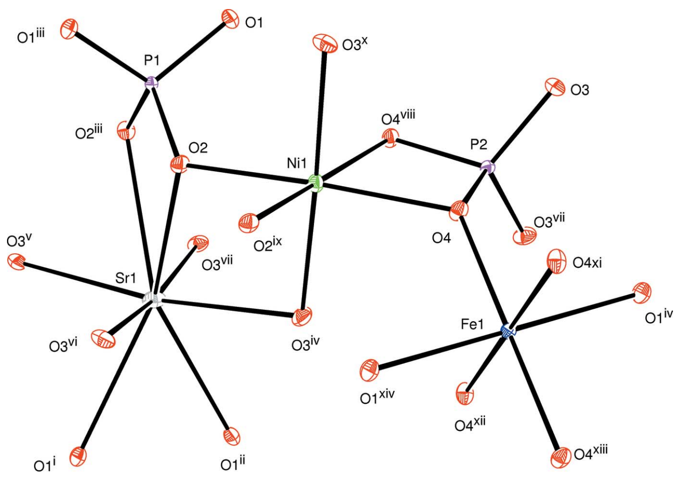

Figure 1
The principal building units in the structure of the title compound. Displacement ellipsoids are drawn at the 50% probability level. [Symmetry codes: (i) $-x + 1, -y + \frac{1}{2}, z - 1$; (ii) $x, y, z - 1$; (iii) $-x + 1, -y + \frac{1}{2}, z$; (iv) $-x + \frac{3}{2}, -y + 1, z - \frac{1}{2}$; (v) $x - \frac{1}{2}, y - \frac{1}{2}, z - \frac{1}{2}$; (vi) $-x + \frac{3}{2}, y - \frac{1}{2}, z - \frac{1}{2}$; (vii) $x - \frac{1}{2}, -y + 1, z - \frac{1}{2}$; (viii) $-x + \frac{3}{2}, y, -z + \frac{3}{2}$; (ix) $-x + \frac{3}{2}, -y + \frac{1}{2}, -z + \frac{3}{2}$; (x) $x, -y + 1, -z + 2$; (xi) $-x + 2, y, z$; (xii) $x, -y + 1, -z + 1$; (xiii) $-x + 2, -y + 1, -z + 1$; (xiv) $x + \frac{1}{2}, y, -z + \frac{3}{2}$.]

and P2 are on 8*g* (*2*), O1 is on 8h (*m*) and O2 is on 8i (*m*)·The three-dimensional network of the crystal structure is composed of two types of layers parallel to (100), as shown in Fig. 2. The first layer is built up from two adjacent edge-sharing octahedra ([Ni_2O_{10}] dimers) whose ends are connected to [PO_4] tetrahedra by a common edge or vertex (Fig. 3). The second layer is formed by an Sr row followed by infinite chains of alternating [PO_4] tetrahedra and [FeO_6] octahedra sharing apices. These two types of layers are linked together by common vertices of [PO_4] tetrahedra, forming a three-dimensional framework which delimits two types of tunnels running along the *a*- and *b*-axis directions in which the Sr cations are located with eight neighbouring O atoms (Fig. 4). The structure of the title compound is isotypic to that of MMn$^{II}_2$Mn^{III}(PO_4)$_3$ (M = Pb, Sr, Ba).

Table 1
Selected bond lengths (Å).

Sr1—O1^{i}	2.6390 (13)	Fe1—O4	1.9703 (8)
Sr1—O2	2.6477 (12)	Fe1—O1^{ii}	2.0751 (12)
Sr1—O3^{ii}	2.6662 (9)	P1—O1	1.5239 (12)
Ni1—O4	2.0561 (8)	P1—O2	1.5514 (12)
Ni1—O2	2.0612 (8)	P2—O3	1.5223 (9)
Ni1—O3^{iii}	2.0953 (9)	P2—O4	1.5722 (9)

Symmetry codes: (i) $-x+1, -y+\frac{1}{2}, z-1$; (ii) $-x+\frac{3}{2}, -y+1, z-\frac{1}{2}$; (iii) $x, -y+1, -z+2$.

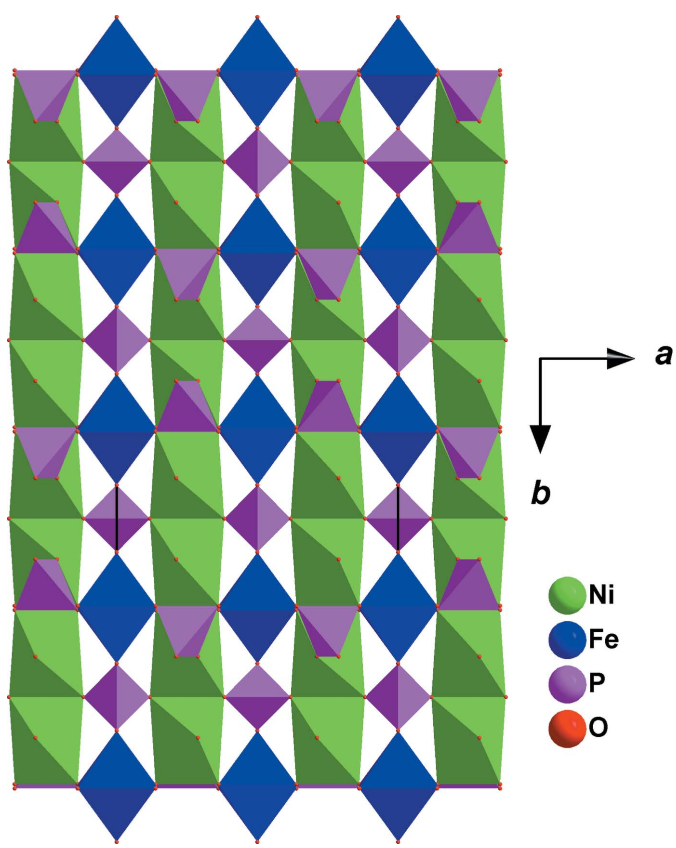

Figure 2
Stacking along [100] of layers building the crystal structure of $SrNi_2Fe(PO_4)_3$.

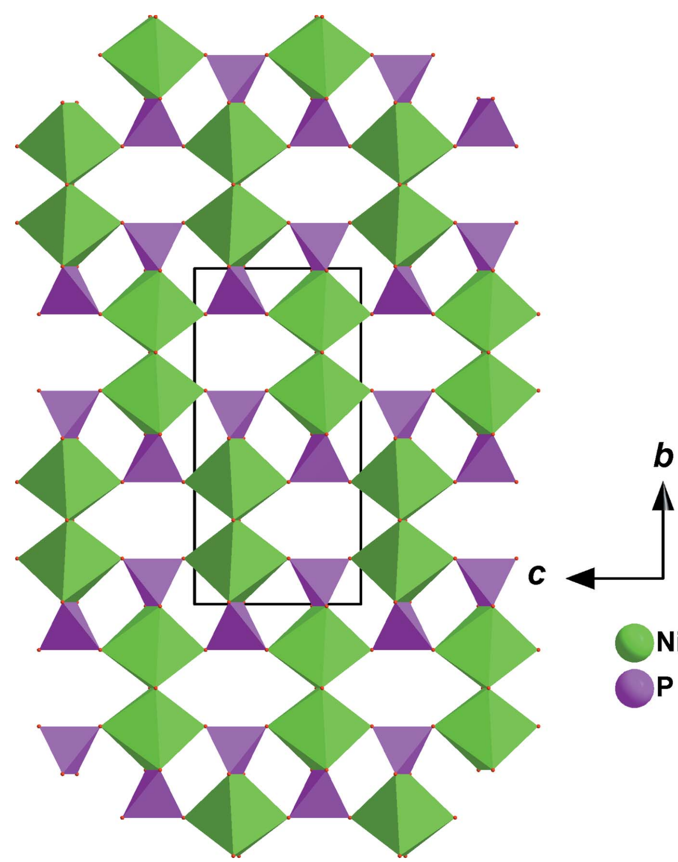

Figure 3
View along the *a* axis of a layer resulting from the connection of [Ni_2O_{10}] dimers and [PO_4] tetrahedra *via* common edges or vertices. Sr cations are omitted.

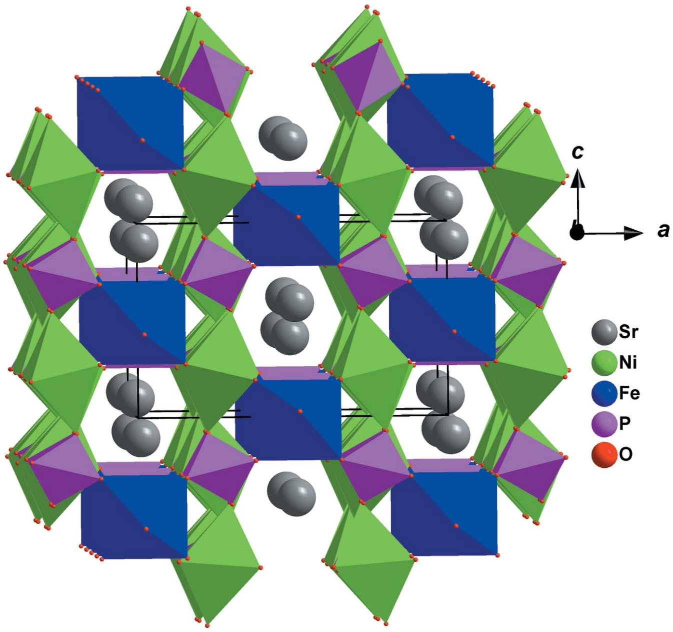

Figure 4
Polyhedral representation of the crystal structure of $SrNi_2Fe(PO_4)_3$ showing tunnels running along [010].

Table 2
Experimental details.

Crystal data	
Chemical formula	$SrNi_2Fe(PO_4)_3$
M_r	545.80
Crystal system, space group	Orthorhombic, *Imma*
Temperature (K)	296
a, *b*, *c* (Å)	10.3881 (11), 13.1593 (13), 6.5117 (7)
V (Å^3)	890.15 (16)
Z	4
Radiation type	Mo *Kα*
μ (mm^{-1})	12.34
Crystal size (mm)	0.31 × 0.25 × 0.19
Data collection	
Diffractometer	Bruker X8 APEX
Absorption correction	Multi-scan (*SADABS*; Bruker, 2009)
T_{min}, T_{max}	0.504, 0.748
No. of measured, independent and observed [$I > 2\sigma(I)$] reflections	8211, 1112, 1095
R_{int}	0.024
$(\sin \theta/\lambda)_{max}$ (Å^{-1})	0.820
Refinement	
$R[F^2 > 2\sigma(F^2)]$, $wR(F^2)$, S	0.015, 0.041, 1.20
No. of reflections	1112
No. of parameters	54
$\Delta\rho_{max}$, $\Delta\rho_{min}$ (e Å^{-3})	0.92, −0.57

Computer programs: *APEX2* and *SAINT* (Bruker, 2009), *SHELXS97* and *SHELXL97* (Sheldrick, 2008), *ORTEP-3 for Windows* (Farrugia, 2012), *DIAMOND* (Brandenburg, 2006), and *publCIF* (Westrip, 2010).

3. Database Survey

It is interesting to compare the crystal structure of α-$CrPO_4$ (Glaum *et al.*, 1986) with that of the title compound. Both phosphates crystallize in the orthorhombic system in the space group *Imma*. Moreover, their unit-cell parameters are nearly the same despite the difference between their chemical formulas. In the structure of α-$CrPO_4$, the Cr^{3+} and P^{5+} cations occupy four special positions and the three-dimensional concatenation of [PO_4] tetrahedra and [CrO_6] octahedra allows the formation of empty tunnels along the *b*-axis direction. We can write the formula of this phosphate as follows: $LL'(Cr1)_2Cr2(PO_4)_3$, and in the general case, $AA'M_2M'(PO_4)_3$ where L and L' represent the two empty tunnels sites, while M and M' correspond to the trivalent cation octahedral sites. This model is in accordance with that of the alluaudite structure which is represented by the general formula $AA'M_2M'(XO_4)_3$ and is closely related to the α-$CrPO_4$ structure (A and A' represent the two tunnels sites which can be occupied by either mono- or divalent medium sized cations, while the M and M' octahedral sites are generally occupied by transition metal cations). Accordingly, the substitution of Cr1 or Cr2 by a divalent cation requires charge compensation by a monovalent cation that will occupy the tunnel. Two very recently reported examples are $Na_2Co_2Fe(PO_4)_3$ and $NaCr_2Zn(PO_4)_3$, which were characterized by X-ray diffraction, IR spectroscopy and magnetic measurements (Souiwa *et al.*, 2015). The replacement of Cr1 by a divalent cation involves an amendment of the charge by a divalent cation as in the present case, $SrNi_2Fe(PO_4)_3$, which is a continuation of our previous work, namely $MMn^{II}_2Mn^{III}(PO_4)_3$ (M = Pb, Sr, Ba).

4. Synthesis and crystallization

$SrNi_2Fe(PO_4)_3$ was synthesized by a solid state reaction in air. Stoichiometric quantities of strontium, nickel, and iron nitrates and 85 wt% phosphoric acid were dissolved in water. The resulting solution was stirred without heating for 20 h and was, subsequently, evaporated to dryness. The obtained dry residue was homogenized in an agate mortar and then progressively heated in a platinum crucible up to 873 K. The reaction mixture was maintained at this temperature during 24 h before being heated to the melting point of 1373 K. The molten product was then cooled down slowly to room temperature at a rate of 5 K h^{-1} rate. Orange parallelepiped-shaped crystals of the title compound were thus obtained.

5. Refinement

Crystal data, data collection and structure refinement details are summarized in Table 2. The highest peak and the deepest hole in the final Fourier map are at 0.72 and 0.80 Å from Sr1 and P1, respectively.

Acknowledgements

The authors thank the Unit of Support for Technical and Scientific Research (UATRS, CNRST) for the X-ray measurements and Mohammed V University, Rabat, Morocco, for financial support.

References

Alhakmi, G., Assani, A., Saadi, M. & El Ammari, L. (2013*a*). *Acta Cryst.* E**69**, i40.

Alhakmi, G., Assani, A., Saadi, M., Follet, C. & El Ammari, L. (2013*b*). *Acta Cryst.* E**69**, i56.

Assani, A., Saadi, M., Alhakmi, G., Houmadi, E. & El Ammari, L. (2013). *Acta Cryst.* E**69**, i60.

Attfield, J. P., Cheetham, A. K., Cox, D. E. & Sleight, A. W. (1988). *J. Appl. Cryst.* **21**, 452–457.

Bouraima, A., Assani, A., Saadi, M., Makani, T. & El Ammari, L. (2015). *Acta Cryst.* E**71**, 558–560.

Brandenburg, K. (2006). *DIAMOND*. Crystal Impact GbR, Bonn, Germany.

Brown, I. D. & Altermatt, D. (1985). *Acta Cryst.* B**41**, 244–247.

Bruker (2009). *APEX2*, *SAINT* and *SADABS*. Bruker AXS Inc., Madison, Wisconsin, USA.

Farrugia, L. J. (2012). *J. Appl. Cryst*. **45**, 849–854.

Glaum, R., Gruehn, R. & Möller, M. (1986). *Z. Anorg. Allg. Chem.* **543**, 111–116.

Huang, W., Li, B., Saleem, M. F., Wu, X., Li, J., Lin, J., Xia, D., Chu, W. & Wu, Z. (2015). *Chem. Eur. J.* **21**, 851–860.

Khmiyas, J., Assani, A., Saadi, M. & El Ammari, L. (2015). *Acta Cryst.* E**71**, 690–692.

Kim, J., Kim, H., Park, K.-Y., Park, Y.-U., Lee, S., Kwon, H.-S., Yoo, H.-I. & Kang, K. (2014). *J. Mater. Chem. A*, **2**, 8632–8636.

Moore, P. B. (1971). *Am. Mineral.* **56**, 1955–1975.

Sheldrick, G. M. (2008). *Acta Cryst.* A**64**, 112–122.

Souiwa, K., Hidouri, M., Toulemonde, O., Duttine, M. & Ben Amara, M. (2015). *J. Alloys Compd.* **627**, 153–160.

Trad, K., Carlier, D., Croguennec, L., Wattiaux, A., Ben Amara, M. & Delmas, C. (2010). *Chem. Mater.* **22**, 5554–5562.

Westrip, S. P. (2010). *J. Appl. Cryst.* **43**, 920–925.

supporting information

Acta Cryst. (2015). E**71**, 1255-1258 [doi:10.1107/S205698901501779X]

Crystal structure of strontium dinickel iron orthophosphate

Said Ouaatta, Abderrazzak Assani, Mohamed Saadi and Lahcen El Ammari

Computing details

Data collection: *APEX2* (Bruker, 2009); cell refinement: *SAINT* (Bruker, 2009); data reduction: *SAINT* (Bruker, 2009); program(s) used to solve structure: *SHELXS97* (Sheldrick, 2008); program(s) used to refine structure: *SHELXL97* (Sheldrick, 2008); molecular graphics: *ORTEP-3 for Windows* (Farrugia, 2012), *DIAMOND* (Brandenburg, 2006); software used to prepare material for publication: *publCIF* (Westrip, 2010).

Strontium dinickel iron orthophosphate

Crystal data

$SrNi_2Fe(PO_4)_3$
M_r = 545.80
Orthorhombic, *Imma*
a = 10.3881 (11) Å
b = 13.1593 (13) Å
c = 6.5117 (7) Å
V = 890.15 (16) Å^3
Z = 4
F(000) = 1044
D_x = 4.073 Mg m^{-3}
Mo *Kα* radiation, λ = 0.71073 Å
Cell parameters from 1112 reflections
θ = 3.1–35.6°
μ = 12.34 mm^{-1}
T = 296 K
Parallelepiped, orange
0.31 × 0.25 × 0.19 mm

Data collection

Bruker X8 APEX Diffractometer
Radiation source: fine-focus sealed tube
Graphite monochromator
φ and ω scans
Absorption correction: multi-scan (*SADABS*; Bruker, 2009)
T_{min} = 0.504, T_{max} = 0.748
8211 measured reflections
1112 independent reflections
1095 reflections with $I > 2\sigma(I)$
R_{int} = 0.024
θ_{max} = 35.6°, θ_{min} = 3.1°
h = −17→17
k = −21→21
l = −9→10

Refinement

Refinement on F^2
Least-squares matrix: full
$R[F^2 > 2\sigma(F^2)]$ = 0.015
$wR(F^2)$ = 0.041
S = 1.20
1112 reflections
54 parameters
0 restraints
$w = 1/[\sigma^2(F_o^2) + (0.0211P)^2 + 1.0433P]$ where $P = (F_o^2 + 2F_c^2)/3$
$(\Delta/\sigma)_{max}$ = 0.001
$\Delta\rho_{max}$ = 0.92 e Å^{-3}
$\Delta\rho_{min}$ = −0.57 e Å^{-3}
Extinction correction: *SHELXL*, $Fc^*=kFc[1+0.001xFc^2\lambda^3/\sin(2\theta)]^{-1/4}$
Extinction coefficient: 0.0040 (3)

Special details

Geometry. All e.s.d.'s (except the e.s.d. in the dihedral angle between two l.s. planes) are estimated using the full covariance matrix. The cell e.s.d.'s are taken into account individually in the estimation of e.s.d.'s in distances, angles and torsion angles; correlations between e.s.d.'s in cell parameters are only used when they are defined by crystal symmetry. An approximate (isotropic) treatment of cell e.s.d.'s is used for estimating e.s.d.'s involving l.s. planes.

Fractional atomic coordinates and isotropic or equivalent isotropic displacement parameters (Å²)

	x	*y*	*z*	U_{iso}*/U_{eq}
Sr1	0.5000	0.2500	0.40652 (3)	0.00832 (6)
Ni1	0.7500	0.36678 (2)	0.7500	0.00507 (6)
Fe1	1.0000	0.5000	0.5000	0.00365 (7)
P1	0.5000	0.2500	0.91246 (8)	0.00335 (9)
P2	0.7500	0.57166 (3)	0.7500	0.00391 (8)
O1	0.5000	0.34416 (9)	1.04869 (19)	0.00631 (18)
O2	0.61817 (11)	0.2500	0.76678 (18)	0.00566 (18)
O3	0.78842 (9)	0.63613 (6)	0.93417 (14)	0.00764 (14)
O4	0.86173 (8)	0.49396 (6)	0.70676 (14)	0.00586 (13)

Atomic displacement parameters (Å²)

	U^{11}	U^{22}	U^{33}	U^{12}	U^{13}	U^{23}
Sr1	0.00864 (10)	0.01114 (10)	0.00518 (9)	0.000	0.000	0.000
Ni1	0.00501 (9)	0.00407 (9)	0.00613 (10)	0.000	0.00049 (6)	0.000
Fe1	0.00281 (12)	0.00403 (12)	0.00410 (12)	0.000	0.000	0.00015 (9)
P1	0.0033 (2)	0.0031 (2)	0.0037 (2)	0.000	0.000	0.000
P2	0.00410 (15)	0.00389 (15)	0.00374 (15)	0.000	0.00042 (10)	0.000
O1	0.0074 (4)	0.0049 (4)	0.0067 (4)	0.000	0.000	−0.0014 (4)
O2	0.0043 (4)	0.0063 (4)	0.0064 (4)	0.000	0.0017 (3)	0.000
O3	0.0095 (3)	0.0080 (3)	0.0055 (3)	−0.0019 (3)	0.0002 (3)	−0.0020 (2)
O4	0.0045 (3)	0.0056 (3)	0.0074 (3)	0.0005 (2)	0.0019 (3)	0.0005 (2)

Geometric parameters (Å, º)

Sr1—O1^{i}	2.6390 (13)	Fe1—O4^{xi}	1.9703 (8)
Sr1—O1^{ii}	2.6390 (13)	Fe1—O4^{xii}	1.9703 (8)
Sr1—O2	2.6477 (12)	Fe1—O4^{xiii}	1.9703 (8)
Sr1—O2^{iii}	2.6477 (12)	Fe1—O4	1.9703 (8)
Sr1—O3^{iv}	2.6662 (9)	Fe1—O1^{xiv}	2.0751 (12)
Sr1—O3^{v}	2.6662 (9)	Fe1—O1^{iv}	2.0751 (12)
Sr1—O3^{vi}	2.6662 (9)	P1—O1	1.5239 (12)
Sr1—O3^{vii}	2.6662 (9)	P1—O1^{iii}	1.5239 (12)
Ni1—O4^{viii}	2.0561 (8)	P1—O2^{iii}	1.5514 (12)
Ni1—O4	2.0561 (8)	P1—O2	1.5514 (12)
Ni1—O2	2.0612 (8)	P2—O3	1.5223 (9)
Ni1—O2^{ix}	2.0612 (8)	P2—O3^{viii}	1.5223 (9)
Ni1—O3^{x}	2.0953 (9)	P2—O4	1.5722 (9)
Ni1—O3^{iv}	2.0953 (9)	P2—O4^{viii}	1.5722 (9)

O1^{i}—Sr1—O1^{ii}	56.01 (5)	O4—Ni1—O3^{x}	92.39 (4)
O1^{i}—Sr1—O2	141.47 (2)	O2—Ni1—O3^{x}	93.49 (4)
O1^{ii}—Sr1—O2	141.47 (2)	O2^{ix}—Ni1—O3^{x}	84.94 (4)
O1^{i}—Sr1—O2^{iii}	141.47 (2)	O4^{viii}—Ni1—O3^{iv}	92.39 (4)
O1^{ii}—Sr1—O2^{iii}	141.47 (2)	O4—Ni1—O3^{iv}	89.31 (3)
O2—Sr1—O2^{iii}	55.24 (5)	O2—Ni1—O3^{iv}	84.94 (4)
O1^{i}—Sr1—O3^{iv}	108.88 (2)	O2^{ix}—Ni1—O3^{iv}	93.49 (4)
O1^{ii}—Sr1—O3^{iv}	78.22 (2)	O3^{x}—Ni1—O3^{iv}	177.91 (5)
O2—Sr1—O3^{iv}	63.76 (3)	O4^{xi}—Fe1—O4^{xii}	180.0
O2^{iii}—Sr1—O3^{iv}	108.81 (3)	O4^{xi}—Fe1—O4^{xiii}	86.39 (5)
O1^{i}—Sr1—O3^{v}	78.22 (2)	O4^{xii}—Fe1—O4^{xiii}	93.61 (5)
O1^{ii}—Sr1—O3^{v}	108.88 (2)	O4^{xi}—Fe1—O4	93.61 (5)
O2—Sr1—O3^{v}	108.81 (3)	O4^{xii}—Fe1—O4	86.39 (5)
O2^{iii}—Sr1—O3^{v}	63.76 (3)	O4^{xiii}—Fe1—O4	180.00 (3)
O3^{iv}—Sr1—O3^{v}	172.25 (4)	O4^{xi}—Fe1—O1^{xiv}	93.70 (3)
O1^{i}—Sr1—O3^{vi}	78.22 (2)	O4^{xii}—Fe1—O1^{xiv}	86.30 (3)
O1^{ii}—Sr1—O3^{vi}	108.88 (2)	O4^{xiii}—Fe1—O1^{xiv}	86.30 (3)
O2—Sr1—O3^{vi}	63.76 (3)	O4—Fe1—O1^{xiv}	93.70 (3)
O2^{iii}—Sr1—O3^{vi}	108.81 (3)	O4^{xi}—Fe1—O1^{iv}	86.30 (3)
O3^{iv}—Sr1—O3^{vi}	68.39 (4)	O4^{xii}—Fe1—O1^{iv}	93.70 (3)
O3^{v}—Sr1—O3^{vi}	111.05 (4)	O4^{xiii}—Fe1—O1^{iv}	93.70 (3)
O1^{i}—Sr1—O3^{vii}	108.88 (2)	O4—Fe1—O1^{iv}	86.30 (3)
O1^{ii}—Sr1—O3^{vii}	78.22 (2)	O1^{xiv}—Fe1—O1^{iv}	180.00 (7)
O2—Sr1—O3^{vii}	108.81 (3)	O1—P1—O1^{iii}	108.80 (10)
O2^{iii}—Sr1—O3^{vii}	63.76 (3)	O1—P1—O2^{iii}	110.85 (3)
O3^{iv}—Sr1—O3^{vii}	111.05 (4)	O1^{iii}—P1—O2^{iii}	110.85 (3)
O3^{v}—Sr1—O3^{vii}	68.39 (4)	O1—P1—O2	110.85 (3)
O3^{vi}—Sr1—O3^{vii}	172.25 (4)	O1^{iii}—P1—O2	110.85 (3)
O4^{viii}—Ni1—O4	71.02 (5)	O2^{iii}—P1—O2	104.61 (9)
O4^{viii}—Ni1—O2	102.98 (3)	O3—P2—O3^{viii}	112.25 (7)
O4—Ni1—O2	171.55 (4)	O3—P2—O4	108.06 (5)
O4^{viii}—Ni1—O2^{ix}	171.55 (4)	O3^{viii}—P2—O4	114.51 (5)
O4—Ni1—O2^{ix}	102.98 (3)	O3—P2—O4^{viii}	114.51 (5)
O2—Ni1—O2^{ix}	83.59 (5)	O3^{viii}—P2—O4^{viii}	108.06 (5)
O4^{viii}—Ni1—O3^{x}	89.31 (3)	O4—P2—O4^{viii}	98.87 (6)

Symmetry codes: (i) $-x+1, -y+1/2, z-1$; (ii) $x, y, z-1$; (iii) $-x+1, -y+1/2, z$; (iv) $-x+3/2, -y+1, z-1/2$; (v) $x-1/2, y-1/2, z-1/2$; (vi) $-x+3/2, y-1/2, z-1/2$; (vii) $x-1/2, -y+1, z-1/2$; (viii) $-x+3/2, y, -z+3/2$; (ix) $-x+3/2, -y+1/2, -z+3/2$; (x) $x, -y+1, -z+2$; (xi) $-x+2, y, z$; (xii) $x, -y+1, -z+1$; (xiii) $-x+2, -y+1, -z+1$; (xiv) $x+1/2, y, -z+3/2$.